arXiv:physics/0403141v1 [physics.atom-ph] 30 Mar 2004

Proposal for high-precision Atomic Parity Violation measurements using amplification of the asymmetry by stimulated emission in a transverse $\vec{E}$ and $\vec{B}$ field pump-probe experiment

J. Guéna, M. Lintz and M. A. Bouchiat *
Laboratoire Kastler Brossel [a] *et Fédération de Recherche* [b]
Département de Physique de l'Ecole Normale Supérieure,
24 Rue Lhomond, F-75231 Paris Cedex 05, France
(February 2, 2008)

Amplification by stimulated emission of radiation provides an intriguing means for increasing the sensitivity of Atomic Parity Violation (APV) measurements in a pump-probe configuration well adapted to the $6S-7S$ cesium transition. It takes advantage of the large number of atoms excited along the path of the pump beam. In the longitudinal E- field configuration currently exploited in an ongoing APV measurement, this number is limited only by the total voltage sustainable by the Cs vapor. In order to overcome this limit, we consider, both theoretically and experimentally, the possibility of performing the measurements in *a transverse E-field* configuration requiring a much lower voltage. We discuss the necessarily different nature of the observable and the magnetoelectric optical effects entering into play. They condition modifications of the experimental configuration with, in particular, the application of a transverse magnetic field. We suggest the possibility of rotating the transverse direction of the fields so as to suppress systematic effects. With *a long interaction length*, a precision reaching 0.1% in a quantum noise limited measurement can be expected, now limited only by the necessity of operating below the threshold of spontaneous superradiant emission of the excited medium. If we approached this limit, however, we could greatly amplify the asymmetry using *triggered* superradiance. PACS numbers: 32.80.Ys, 11.30.Er, 33.55.b

I. INTRODUCTION

A. Motivation for new independent measurements

The main goal of Atomic Parity Violation (APV) experiments is a precise determination of Q_W, the so-called weak charge of the nucleus which, as far as the electron-nucleus weak interaction is concerned, plays the same role as the electric charge for the Coulomb interaction [1]. The value of $Q_W(Cs)$ is quoted as a significant constraint on "New Physics" in the Particle Data Book [2]. Atomic calculations in cesium have reduced their uncertainty below 1% [3] and many cross checks have reinforced confidence in the results at this level [4–6]. On the experimental side a single group [7,8] has met the challenge which consists in achieving a calibrated [9] measurement of the APV $6S-7S$ transition amplitude E_1^{pv} at a level of precision better than 1%. However, the measurement of any fundamental quantity has to pass the test of the verification by a completely independent method. Moreover, it has been reemphasized recently [10,11] that their reported value for the small nuclear spin-dependent contribution is difficult to explain theoretically.

APV experiments are notoriously difficult from the standpoints of both low statistics and the possibility of numerous systematic effects. Solutions which increase the Signal to Noise Ratio (SNR) often give rise to undesirable spurious effects. In our first Cs APV Stark interference experiment [12], the detection method was selective but inefficient. The same was true for APV measurements in thallium [13]. Conversely, in the atomic beam experiments on Cs [7], the SNR is huge by comparison, thanks to the high light intensity obtained in the power build-up cavity. However, this is at the price of non-linear effects which complicate interpretation of the data.

B. Interesting features of a pump-probe experiment

More recently, another method [14] has provided its first APV measurements [15], and highlighted a mechanism looking attractive as regards its potential gain of sensitivity, namely amplification by stimulated emission of radiation [16]. It relies on a pump-probe scheme in which the excited $7S$ state is populated by an intense, pulsed excitation beam, with a linear polarization $\hat{\epsilon}_{ex}$ and a wave vector $\hat{k}$ parallel to the applied electric field $\vec{E}$. The atoms are then probed by a second, collinear pulsed laser beam which is tuned to resonance for the $7S \rightarrow 6P_{3/2}$ transition. The probe beam is amplified by stimulated emission. At the same time its linear polarization $\hat{\epsilon}_{pr}$, undergoes a small change of direction or pseudo-rotation, due to a linear dichroism arising from the presence of the pseudoscalar term $(\hat{\epsilon}_{ex}\cdot\hat{\epsilon}_{pr})(\hat{\epsilon}_{ex}\wedge\hat{\epsilon}_{pr}\cdot\vec{E})$ in the gain and leading to a tilt θ^{pv} of its eigen-axes with respect to the planes of symmetry of the experiment [15,20]. This tilt is given by the ratio of the PV E_1 amplitude to the vector part of the Stark induced amplitude [1] $\theta^{pv} = -\mathrm{ImE}_1^{\mathrm{pv}}/\beta E$, about 1 μrad in current experimental conditions. This is the important parameter to be measured. We note that the pseudo-rotation of $\hat{\epsilon}_{pr}$ is, as θ^{pv}, odd under $\vec{E}$ reversal, which provides a powerful tool for discriminating against systematic effects. We measure the rotation with a high sensitivity, two-channel polarimeter operating in balanced mode [21], in which it gives rise to an imbalance $D_{amp} = \frac{S_1-S_2}{S_1+S_2}$ between the signals, S_1, S_2 recorded in the two channels

detecting the *amplified* probe beam. To reject the contribution due to imperfections of the probe polarization, the imbalance is also measured with a subsequent *reference* probe pulse and subtracted [17] to yield, at each excitation pulse, the imbalance of atomic origin, that is the left-right asymmetry: $A_{LR} \equiv D_{at} = D_{amp} - D_{ref}$. Using real-time calibration by a known tilt of the optical axes of parity-conserving origin, we deduce the value of θ^{pv}.

We have already demonstrated that this method has a good detection efficiency (all photons arising from stimulated emission by the probe beam reach the polarimeter) while preserving the selectivity of the fluorescence detection approach. In addition, this scheme allows us to exploit rotational symmetry about the pump probe common beam axis to reduce systematic effects [22]. The limit of sensitivity achievable by our present technique is the important issue at stake, discussed in this paper. The SNR is definitely better than that obtained using polarized fluorescence detection and it is expected to bring us to within reach of our 1% precision objective. However, one should not conclude that this represents the ultimate sensitivity limit obtainable with the stimulated-emission method of detection. Indeed the key point here is that we use an enhancement mechanism which considerably increases both the probe intensity *and* its left-right asymmetry with the optical density at the probe wavelength. Since we first validated the method [15], we have checked that this mechanism does really increase the SNR. It has indeed contributed significantly to the increase by a factor of 3.3 that we have recently obtained. This raises the question of just how much more one might expect to increase the sensitivity in this way.

C. Practical limit to the amplification with a longitudinal $\vec{E}$ field

The optical density of the Cs vapor at the probe wavelength $\mathcal{A} = \ln(n_{out}/n_{in})$, deduced from the number of incoming (n_{in}) and outgoing (n_{out}) probe photons, is proportional to the number of $7S$ excited atoms in the interaction region N, itself proportional to the excitation beam energy, to the square of the electric field strength E^2 and to the length of the cell. At the quantum limit, the inverse of the noise equivalent angle $NEQA$ per pulse, hence the measurement sensitivity, involves the square root of the number of probe photons per pulse reaching the detector, $n_{in}\exp(\mathcal{A})$, times the asymmetry amplification factor [16], $dA_{LR}/d\theta$. This result [18] relies on two reasonable assumptions that we wish to make explicit here. First, the polarimeter operates in balanced mode. Second, the number of collected photons spontaneously emitted in the mode of the probe beam is very small as compared to the number of stimulated photons ($\simeq 10^{-6}$ in typical conditions), and remains small at moderate amplifications, so that the associated noise can be neglected [19].

In the limit $\mathcal{A} \leq 1$, the asymmetry amplification can be expressed in an identical way for both the "para" ($\hat{\epsilon}_{ex} \parallel \hat{\epsilon}_{pr}$), and "ortho" ($\hat{\epsilon}_{ex} \perp \hat{\epsilon}_{pr}$), configurations:

$$dA_{LR}/d\theta = 2\eta_{av}\mathcal{A}_{av} \quad , \tag{1}$$
$$\text{with} \quad \mathcal{A}_{av} = (\mathcal{A}_{\parallel} + \mathcal{A}_{\perp})/2 \quad \text{and} \quad \eta_{av} = \frac{\alpha_{\parallel} - \alpha_{\perp}}{\alpha_{\parallel} + \alpha_{\perp}} \, ,$$

where $\mathcal{A}_{\parallel}$ and $\mathcal{A}_{\perp}$ denote the optical densities and $\alpha_{\parallel}$ and $\alpha_{\perp}$ the amplification coefficients for the field per unit length, in the two configurations [16]. For the favorable $6S_{F=3} \rightarrow 7S_{F=4} \rightarrow 6P_{3/2,F=4}$ transition $2\eta_{av} = 22/23$, which henceforth we approximate by 1. Thus we can write:

$$(NEQA)^{-1} = \sqrt{n_{in}}\exp(\mathcal{A}_{av}/2) \times \mathcal{A}_{av} \, , \tag{2}$$

which obviously corresponds to a rapid increase of the quantum noise limited SNR $= \theta^{pv}(NEQA)^{-1}$/pulse as a function of $\mathcal{A}$.

In the longitudinal field configuration, where $\vec{E}_{\parallel}$ lies along the common beam direction $\hat{k}$, the only parameter left in our experiment for increasing $\mathcal{A}$ is the excitation beam intensity. To increase the applied electric field we need to increase the applied potentials but at the large Cs vapor densities at which we operate (a few times $10^{14}/\text{cm}^3$), too large a voltage would present the risk of a discharge inside the vapor. With $\vec{E} \parallel \hat{k}$, increasing the length also requires a prohibitive increase of the applied voltage. By contrast, this kind of limitation is obviously absent if the experiment is performed not in the longitudinal but in the *transverse* field configuration. We also note that in a transverse field $\vec{E}_{\perp}$, the left-right PV asymmetry receives a contribution not only from the vector Stark induced amplitude $i\beta\vec{E}_{\perp} \wedge \vec{\sigma} \cdot \hat{\epsilon}_{ex}$ (where $\vec{\sigma}$ denotes the electron spin operator) but also from the scalar one $\alpha\vec{E}_{\perp} \cdot \hat{\epsilon}_{ex}$. For the $6S \rightarrow 7S$ Cs transition [1], $|\alpha| \simeq 10\,|\beta|$. Therefore, at smaller field magnitudes $E_{\perp}$, typically close to $E_{\parallel}/10$, and with a longer interaction length, we can expect an overall left-right asymmetry significantly larger than in the longitudinal field configuration. However, the physical quantity which bears the PV signature in a transverse E-field is different. We examine it in detail in the next section.

II. A PUMP-PROBE APV EXPERIMENT IN A TRANSVERSE ELECTRIC FIELD

A. The need for a magnetic field

While in a longitudinal $\vec{E}$ field the observables are the different contributions to the $7S$-excited alignment [22], detected through the linear dichroism or birefringence to

which they give rise, in the transverse $\vec{E}$ field geometry the observables are the contributions to the $7S$ orientation giving rise to circular dichroism or optical rotation. However, only the orientation component $\vec{P}\cdot\hat{k}$ collinear to the beam contributes to the probe polarization signal. We show below that it is possible to realize conditions such that, at least in principle, only the orientation of parity violating origin participates to the signal.

There are several contributions to the orientation created in the $7S$ state. The interference between the Stark-induced electric-dipole transition amplitudes of scalar and vector origins gives rise to a longitudinal component $\vec{P}^{(2)} = -\frac{5}{6}\frac{\beta}{\alpha}\xi_{ex}\hat{k}$, where ξ_{ex} denotes the photon helicity. In addition, the interference of the scalar Stark-induced amplitude with the magnetic-dipole amplitude M_1 on the one hand and the parity violating electric-dipole amplitude $\mathrm{Im}\mathrm{E}_1^{\mathrm{pv}}$ on the other, gives rise to the transverse component:

$$\vec{P}_\perp = \frac{5}{6}\frac{M_1 + \xi_{ex}\mathrm{Im}\,\mathrm{E}_1^{pv}}{\alpha E_\perp}(\hat{k}\wedge\hat{E}_\perp) \equiv \vec{P}^{(1)} + \vec{P}^{pv}, \quad (3)$$

after excitation of the $6S_{F=4} \rightarrow 7S_{F=4}$ line. We have split $\vec{P}_\perp$ into the PV contribution $\vec{P}^{pv}$ and the M_1 contribution $\vec{P}^{(1)}$ which is 2×10^4 larger, but which cancels out if the atoms are excited by two counterpropagating beams of equal intensity [23] (see Fig.1).

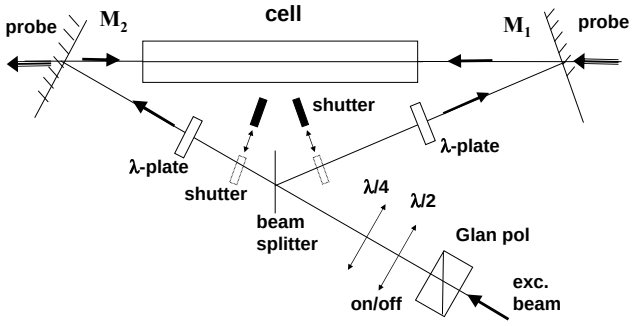

FIG. 1. Schematic of the optical arrangement allowing for the cancellation of $\vec{P}^{(1)}$: two counterpropagating excitation beams are made colinear to the probe beam by using dichroic mirrors (M_1, M_2); their extinction is monitored by two independent shutters. The birefringences on the two paths are corrected by adjusting the axis orientation and the tilt of two λ-plates.

Since the $\mathrm{Im}\,\mathrm{E}_1^{\mathrm{pv}}$ contribution we want to observe is perpendicular to $\hat{k}$ and to $\vec{E}_\perp$, we apply a magnetic field $\vec{B}$ in the direction parallel to $\vec{E}_\perp$. We also delay the probe pulse with respect to the excitation pulse to give the transverse orientation created sufficient time to precess around $\vec{B}$ towards the direction of the beam $\hat{k}$. Simultaneously, the component $\vec{P}^{(2)}$ precesses by the same angle and becomes orthogonal to $\hat{k}$. If the instants of excitation and detection for all atoms coincided, we would expect the simple time-dependences $\sin(\omega_L t)$ for $\vec{P}^{pv}$ and $\cos(\omega_L t)$ for $\vec{P}^{(1)}$. By numerically averaging over realistic time distributions we find the predicted time-dependence is still described by a sine and a cosine law to within a good approximation, if one replaces the Larmor angular precession frequency ω_L of one atom in the applied $\vec{B}$ field by an effective angular frequency ω_{eff} whose numerical value depends on experimental parameters such as excitation pulse duration and probe intensity.

B. Dark-field detection

During an exploratory stage of the experiment [25], we have observed the B-field dependence of $\vec{P}^{(1)}\cdot\hat{k}$ and $\vec{P}^{(2)}\cdot\hat{k}$ (Fig.2). We have found that the field magnitude required to suppress the $\vec{P}^{(2)}\cdot\hat{k}$ Stark-induced longitudinal contribution is 28 G for an excitation-probe pulse delay of 20 ns, *i.e.* sufficiently short to avoid significant loss of excited atoms by spontaneous decay. Another important feature is that, for that delay, the magnitude of $\vec{P}^{(1)}$ observed with a single excitation beam is very close to its maximum value. Therefore, adjustment of both the delay and the field magnitude combined with the use of two counter-propagating beams enables us to ensure dark-field detection of $\vec{P}^{pv}$. We have verified that, over durations as short as 20 ns, the damping of the 7S polarization due to collisional relaxation is completely negligible.

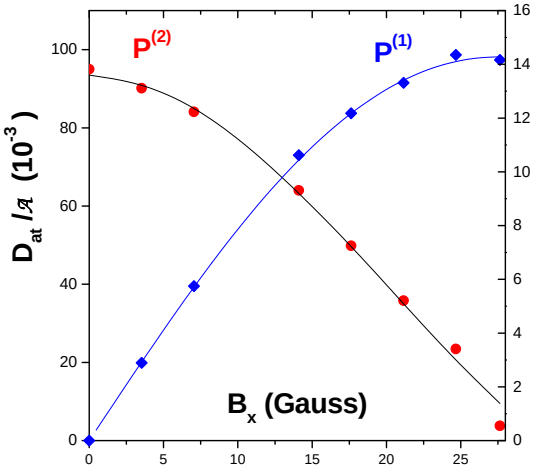

FIG. 2. Larmor precession of $\vec{P}^{(1)}$ and $\vec{P}^{(2)}$ in a magnetic field $\vec{B}$ parallel to $\vec{E}_\perp$, observed in real time with a single excitation beam: the pump-probe delay is kept fixed at 20 ns and the magnitude of the field is varied. $\vec{P}^{(1)}\cdot\hat{k}$ (diamonds, right scale) and $\vec{P}^{(2)}\cdot\hat{k}$ (dots, left scale) are deduced from the contributions to $D_{at}/\mathcal{A}$ (for definitions see the text) respectively ξ_{ex}-even, $E_\perp$-odd, B-odd and ξ_{ex}-odd, $E_\perp$-even, B-even. ($E_\perp$= 185 V/cm; exc. pulse 0.9 mJ; resonant for $6S_{F=4} \rightarrow 7S_{F=4}$; beam diameter 1.8 mm; probe pulse, 4×10^7 linearly polarized ($\parallel \vec{B}$) photons, resonant for $7S_{F=4} \rightarrow 6P_{3/2,F=5}$) [25].

The linearly polarized resonant probe beam passing through the oriented vapor acquires a small helicity. For sensitive detection of this helicity we have converted our two-channel polarimeter [21] from a linear to a circular analyzer by inserting a quarter wave plate in front of the polarizing beam splitter cube. The imbalance of atomic origin is still defined as $D_{at} = D_{amp} - D_{ref}$. The tiny contribution to D_{at} which is odd under the reversals of ξ_{ex}, $\vec{E}$ and $\vec{B}$ provides us with the PV observable, $\vec{P}^{pv} \cdot \hat{k}$. An important step is to normalize it by another imbalance of well known atomic origin serving as a calibration. For this purpose, we can use the imbalances occuring when one or the other of the two counterpropagating excitation beams is blocked. They provide us with the observable $\vec{P}^{(1)} \cdot \hat{k}$. Thereby we can extract directly $\mathrm{Im}\,\mathrm{E}_1^{pv}/M_1$ from the ratio of the E-odd atomic imbalance measured with both excitation beams present, $D^{at}(\hat{k}_{ex}, -\hat{k}_{ex})$, to the difference of the E-odd imbalances obtained with a single excitation beam present, $D^{at}(\hat{k}_{ex}) - D^{at}(-\hat{k}_{ex})$. It is interesting to note that this normalization procedure has the advantage of eliminating the magnitude of the electric field. However, because of the asymmetry amplification process, for precise measurements it is important to measure all the imbalances to be compared at equal optical densities. One simple way to fulfill this condition for measurements made alternatively with a single beam or two beams, might consist in increasing the applied potential for a single beam so as to double $E_\perp^2$, the extracted quantity then being $\sqrt{2}\,(\mathrm{Im}\,\mathrm{E}_1^{pv}/M_1)$.

It can be recalled that a PV asymmetry of the same origin has already been observed in our group, though in very different experimental conditions, using polarized fluorescence detection [12]. This earlier work provides valuable information: our detailed analysis of the main systematic effects [26], transposed to the present situation, allows us to evaluate the risks of systematic effects in this new detection scheme. As confirmed by other transverse field PV experiments, the most troublesome source of systematics arises from interference between the Stark-induced electric-dipole and the magnetic-dipole amplitudes. Thanks to the use of two counterpropagating beams, there are two criteria to discriminate the E_1^{pv} against the M_1 contribution, based on their different behaviour under ξ_{ex} and $\hat{k}_{ex}$ reversals. However this is not enough to guarantee the absence of systematic effects at the level needed for reaching a high accuracy. Indeed, if the cell input window has a birefringence $\alpha_{ex}^{(1)}$ with its axes at 45° to $\vec{E}_\perp$, then the $6S-7S$ excitation rate is affected by a ξ_{ex}-dependent contribution, the vapor acting like a linear analyzer oriented along the direction of $\hat{E}_\perp$, which detects $|\hat{E}_\perp \cdot \hat{\epsilon}_{ex}|^2 = (\frac{1}{2} - \alpha_{ex}^{(1)}\,\xi_{ex}\,)$. To first approximation this contribution is the same for the $7S$ population and the $7S$ polarization signals, respectively proportional to $\mathcal{A}$ and D_{at}, so that it cancels in their ratio. However, as soon as the contributions to the transition rate proportional to $\alpha\beta$ and β^2 are taken into account this compensation is no longer exact and in the ratio $D_{at}/\mathcal{A}$, the birefringence problem is not eliminated, but reduced at the level of $2\alpha_{ex}^{(1)}\kappa$ (where $\kappa = -\frac{\beta}{4\alpha} + \frac{5\beta^2}{6\alpha^2} \simeq 3\times10^{-2}$). With $2\alpha_{ex}^{(1)} = 10^{-3}$ rad, the systematic effect would be $3\times10^{-5}\times P^{(1)}$, or 60% of the PV signal itself. Clearly other means of discrimination are necessary.

C. Recovering the axial symmetry

A further efficient way to suppress this source of systematics would be to exchange the direction of the fast and slow axes of birefringence with respect to the direction of $\vec{E}_\perp$. Since this looks unfeasible with a cesium vapor cell, we have considered instead the possibility of rotating the field by 90°, which is of course equivalent. We propose a new design of the electrodes (Fig. 3) such that by simply switching voltages and currents the measurement can be repeated with both $\vec{E}_t$ and $\vec{B}$ fields rotated by 90°. This is equivalent to switching the sign of $\alpha_{ex}^{(1)}$, so that the ξ_{ex}-dependent contribution to $P^{(1)}$ due to $\alpha_{ex}^{(1)}$ also changes sign. Owing to this additional reversal we expect to improve the discrimination between P^{pv} and $P^{(1)}$ by more than two orders of magnitude. As shown in Fig. 3, it is even possible to perform rotations of $\vec{E}_\perp$ by successive increments of 45°. First, this provides a sensitivity to the birefringence $\alpha_{ex}^{(3)}$ having its axes parallel and orthogonal to $\vec{E}_\perp$ via the observation of the ξ_{ex} dependence of $\mathcal{A}$ once $\vec{E}_t$ is rotated by 45°. Second, since $\alpha_{ex}^{(3)}$ can combine with a small misalignment of $\vec{E}_\perp$ and $\vec{B}$ to generate a systematic effect, the possibility of alternating measurements in two orthogonal directions of $\vec{E}_\perp$ are here again very helpful.

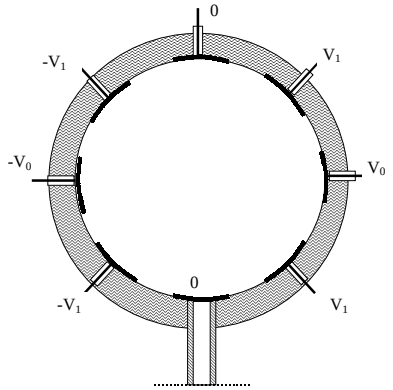

FIG. 3. Electrode arrangement inside a cylindrical cell allowing one to rotate the transverse electric field by increments of 45°. We have shown by numerical simulation that, by adjusting the potential ratio V_1/V_0, we could make the field very homogeneous close to the axis. The side arm is to be connected to the Cs reservoir (not shown).

The cell should be made from an insulating material, for instance high purity alumina to which sapphire windows can be glued [27]. In our preliminary measurements, following ideas similar to those exploited for realizing the longitudinal field configuration [28], we used an alumina cell with *external* electrodes. The design of Fig.3 with *internal electrodes* would provide the possibility to eliminate the electric charges induced by photoionization of the sapphire windows under the impact of the intense excitation pulse [22]. However, it should be noted that, as confirmed by observation, the transverse field configuration favours a reduction of space charge effects. Indeed, due to its direction the field tends to drag all the free electrons out of the interaction region. In addition if the cell length is increased, for a given excitation energy the relative importance of the space charge effects located close to the windows will be reduced.

At a first glance, the transverse field pump-probe experiment appears to lack cylindrical symmetry, one of the main advantages inherent to the longitudinal E-field geometry. In actual fact, we can recover this symmetry by using the electrode configuration proposed in Fig.3 which makes it possible to alternate measurements with directions of the transverse E-field rotated by angular increments of 45° and directions of $\vec{B}$ simultaneously rotated by adjusting the currents in two pairs of coils. We mention that signals of atomic origin permit to test the defect of parallelism between $\vec{E}$ and $\vec{B}$ in each configuration [29].

III. EXPECTED GAIN OF SENSITIVITY WITH $\vec{E}$ TRANSVERSE

A. Estimated gain

Now we have defined the operating conditions necessary for obtaining dark-field detection of a calibrated PV asymmetry having a very specific signature in the transverse field configuration, we can discuss at last the crucial objective at stake: how to increase the experimental sensitivity by making use of the asymmetry amplification given by a longer interaction length. To estimate the SNR ratio for the polarimeter operating as a circular polarization analyzer we use the simplified model already employed to discuss asymmetry amplification in the $\vec{E}_{\|}$ configuration [16]. It provides clear analytical results for $dA_{LR}/d\theta$ and although we used it somewhat beyond its range of validity (rather large saturation levels, short probe pulse durations), we have found that its predictions reproduce our observations well, not only their general trend but even semi-quantitatively [18]. (Note that numerical methods to arrive at quantitative predictions in specific conditions, if need be, have also been given in [16], but they lead to less transparent results). Transposing to the transverse field experiment the reasoning leading to Eq. 1, we derive the expression of the Noise Equivalent Polarization, $NEQP$, at the limit of quantum noise:

$$(NEQP)^{-1} = \sqrt{n_{in}} \exp\left(\mathcal{A}(E_\perp)/2\right) \times dA_{LR}/dP. \quad (4)$$

Since P^{pv} is in the range of 10^{-6}, the left-right asymmetry $A_{LR} \equiv D_{at} = \frac{1}{2}(\exp\left(\mathcal{A}\zeta P\right) - \exp\left(-\mathcal{A}\zeta P\right))$ can be written simply as $A_{LR} \simeq \mathcal{A}\zeta P$, which exhibits the sensitivity of A_{LR} to measuring the $7S$ orientation. ζ is an angular coefficient depending on the probe transition, 6/5 in the favorable case of the $7S_{F=4} \rightarrow 6P_{3/2,F=5}$ transition.

Writing explicitly the dependence of $\mathcal{A}(E_\perp)$ on the adjustable parameters, $\mathcal{A}(E_\perp) = k\alpha^2 E_\perp^2 L_\perp$, such as the field magnitude and the cell length, we obtain the SNR/pulse in a transverse field experiment:

$$\begin{aligned} SNR(\vec{E}_\perp) &= |P^{pv}| \times (NEQP)^{-1}, \\ &= k\mathrm{Im}E_1^{pv} \alpha E_\perp L_\perp \exp\left(\frac{k}{2}\alpha^2 E_\perp^2 L_\perp\right) \times \sqrt{n_{in}}, \end{aligned} \quad (5)$$

to be compared to the SNR/pulse in a longitudinal field case (where $\mathcal{A}(E_{\|}) \simeq k\beta^2 E_{\|}^2 L_{\|}$, [30]):

$$\begin{aligned} SNR(\vec{E}_{\|}) &= |\theta^{pv}| \times (NEQA)^{-1}, \\ &= k\mathrm{Im}E_1^{pv} \beta E_{\|} L_{\|} \exp\left(\frac{k}{2}\beta^2 E_{\|}^2 L_{\|}\right) \times \sqrt{n_{in}}. \end{aligned} \quad (6)$$

The role of the interaction length is made clear from both Eqs. 5 and 6. Presently $L_{\|} = 8$ cm, let us suppose that we can operate with $L_\perp = 40$ cm and $E_\perp = \frac{\beta}{\alpha} E_{\|}$, we can then reasonably expect:

$$SNR(E_\perp) = \frac{40}{8} \exp\left(\frac{\mathcal{A}(E_\perp)}{2} - \frac{\mathcal{A}(E_{\|})}{2}\right) \times SNR(E_{\|}). \quad (7)$$

With $\mathcal{A}(E_{\|}) \simeq 0.4$ and $\mathcal{A}(E_\perp) \simeq 2.0$, Eq.7 predicts a sensitivity gain by a factor of $\simeq 5 \times \exp 0.8 = 10$ which, if real, would literally transform the experimental situation. One might wonder about using still larger values of $\mathcal{A}(E_\perp)$ by making L longer or $E_\perp$ larger? In fact, at higher optical density, a new physical process comes into play, namely superradiance.

B. Towards larger optical densities: spontaneous versus triggerred superradiance

At high optical densities $\mathcal{A}$, the excited vapor can superradiate spontaneously within some time delay, which becomes shorter as $\mathcal{A}$ is increased. This process has been the subject to both theoretical and experimental investigations in the past [31–33], and more recently for conditions corresponding to those encountered here [34].

The present situation is particularly well suited for studying superradiance: by smoothly increasing the optical density, for instance with a knob driving the E-field magnitude, it is possible to study the atomic emission as it gradually goes through three different regimes: i) linear amplification of a resonant saturating probe pulse, ii) triggered superradiance, when superradiance emission is triggered by the injection of a weak resonant probe pulse and iii) spontaneous superradiance occuring without any probe beam, within a delay τ_D . In a first approximation, the delay of the onset of spontaneous superradiance is inversely proportional to the number of excited atoms in the interaction region N and hence to $\mathcal{A}$:

$$\tau_D = \frac{8\pi}{3}\frac{a^2}{N\lambda^2\Gamma}\log N\,. \tag{8}$$

Here a is the diameter of the excitation beam, λ the wavelength of the probe transition and Γ is the spontaneous emission rate for the most probable hyperfine component. Because of the near-absence of Doppler dephasing between the dipoles, due to the narrow spectral width of the excitation laser, the threshold is nearly as low as Eq.8 predicts which is not the case in many other practical circumstances. However, we must bear in mind that the measurements reported in [34] were performed without any applied magnetic field. We expect such a field to cause dephasing and hence delay the superradiant emission. Consequently, the values of τ_D recorded versus the number of excited atoms, presented in [34] only serve as a *lower limit* to estimate the delay as a function of $\mathcal{A}$ in the conditions of this proposal.

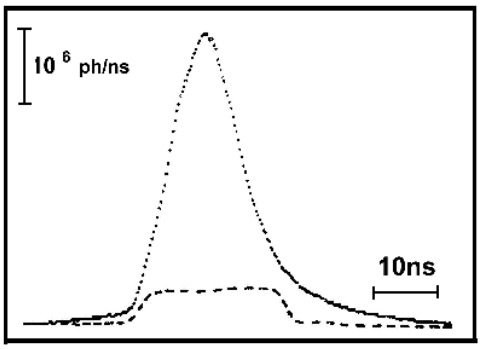

FIG. 4. Example of a triggered superradiant pulse. Dashed curve: the probe pulse (unamplified) in the absence of excited atoms. Dotted curve: due to the presence of excited atoms the probe pulse is amplified. The experimental conditions ($n_{Cs} = 1.8\times10^{14}$ at/cm^3, $E_\perp = 400$ V/cm, $L_\perp$ =25 mm) are such that the optical density is large. Note that a non-zero intensity is observable even before the probe gate is opened. This is due to the photon leakage (a few 10^{-3}) through the "closed" probe gate, which prepares the build-up of the coherence of the atomic dipoles. When the probe gate is opened (80 μW, 20 ns), full triggering of the superradiance occurs without any delay [34].

Actually, for PV measurements τ_D should not be too short (hence $\mathcal{A}$ should not be too large) for two major reasons. First, to observe $\vec{P}^{pv}$, this vector must undergo a Larmor precession and τ_D must be long enough for the precession to have time to occur. Second, the random character of spontaneous superradiance deprives the detection of the stability required to make high precision measurements. Reliable measurements are possible only if the probe pulse can be applied before any superradiance spontaneously occurs.

By contrast, the triggered superradiance regime offers very attractive possibilities: a very weak radiation field is enough to suppress fluctuations in direction, frequency and polarization of the spontaneous emission and to give rise to complete, sudden emission of the whole 7S atom population leading to a *very large amplification of the probe pulse* (see Fig.4). It is still more important to notice that *this is accompanied by an amplification of the left-right asymmetry* resulting from the angular anisotropy (orientation) of the radiating atomic medium [34]. For instance, in a situation close to that of Fig.4 we have observed an asymmetry amplification by a factor of 4. As underlined by Eq.5, such an increase in sensitivity of dA_{LR}/dP would be of invaluable help.

After examination of our data giving τ_D versus $\mathcal{A}$, we arrive at the conclusion that the gain of sensitivity by a factor of 10 predicted from Eq.7 with $\mathcal{A}(E_\perp) = 2.0$, looks realistic, so that the future of high precision APV experiments based on amplification by stimulated emission appear very promising. Using this technique measurements at the precision level of 0.1% look feasible.

IV. AN ALTERNATIVE EXPERIMENTAL APPROACH

Finally, we would like to mention that the experimental configuration depicted in this paper presents an interesting alternative. It can be verified that with an excitation beam *linearly polarized*, and with two *transverse* electric and magnetic fields, which are *orthogonal*, then the excited atoms acquire an orientation in the direction $\vec{E}\wedge\vec{B}$, hence along the direction of the excitation beam. For $\Delta F = 0$ lines, this new observable can be written as $\vec{P}^{pv}(B) \propto \mathrm{Im}E_1^{pv}\alpha\vec{E}\wedge\vec{B}$. Contrary to the situation of section II, where we considered an orientation $\vec{P}^{pv}$ present in absence of B, but requiring the B-field to be detectable by the probe, here we have a new orientation component directly created in the observation direction, but which cancels out when $B = 0$. To observe it one requires partial resolution of the Zeeman structure of the $6S - 7S$ transition which is not difficult in view of the Doppler width reduction obtained in the pump-probe configuration (in a zero magnetic field the linewidth, partly due to the finite excitation duration, is about 80 MHz). This has several advantages: the

PV signal can be observed via dark-field detection, using the differential two-channel polarimeter, *without any pump-probe delay*; thus the risk of spontaneous superradiance is pushed towards higher optical densities. On the $\Delta F = 0$ transitions, with linear polarization $\hat{\epsilon}_{ex}$ chosen parallel to $\vec{E}$, there is no contribution arising from the M_1 amplitude. However to calibrate the $P^{pv}(B)$ signal, a good solution might consist in switching the excitation polarization from linear to circular. With a single excitation beam, the lifting of degeneracy gives rise to a longitudinal polarization of the excited state $\vec{P}^{(1)}(B) \propto \alpha E M_1 \xi_{ex} \vec{E} \wedge \vec{B}$ due to the Stark-M_1 interference, which is detectable in the same conditions as $\vec{P}^{pv}(B)$. The advantage is that, as in the first approach, this calibration gives access directly to $\mathrm{Im}E_1^{pv}/M_1$ independently of the E-field magnitude and independently of the line shape. Note that, experimentally, there can be no confusion with the transverse orientations $\vec{P}^{(1)}$ and $\vec{P}^{pv}$ discussed in sect. II, Eq.3, since their Larmor precession is blocked by the $\vec{B}$-field now parallel to the direction along which they are created.

Moreover, let us point out that all that has been said in the preceding discussion about the risks of systematic effects connected with window birefringence and the ways to eliminate them, can be transposed to this configuration. In particular a rotation of the transverse fields around the common beam direction is well adapted to overcoming the window birefringence.

Due to its physical origin linked to partial resolution of the Zeeman structure, this orientation signal exhibits a line shape which is an odd function of the frequency detuning of the excitation beam with respect to the probe beam frequency, and passes through zero close to resonance. The same result also holds if the signal observed is the circular dichroism of the probe. In these conditions, one might prefer to observe the optical rotation signal which is an even function of the frequency detuning [35].

V. CONNECTIONS WITH PREVIOUS WORK

In this section we would like to point out that the study of E-field assisted forbidden transitions and the search for atomic parity violation based on probe-beam detection, has opened up a wide class of magnetoelectric optical effects. Up to now, several groups have been interested in the circular or linear dichroism which affect the beam exciting a forbidden transition due to the contribution to the transition rate of an interference between the Stark-induced electric dipole amplitude and either the E_1^{pv} or the M_1 amplitudes. However, the forbidden transition is so weak that the dichroism is not directly detectable on the *transmitted* excitation beam itself. In fact, the *population* of the excited state has been the quantity monitored using fluorescence detection. Thus, the circular dichroism $\propto \xi_{ex} \hat{k} \cdot \vec{E} \wedge \vec{B}$ observed in the APV Cs experiment at Boulder [7] was detected by looking for a change of the fluorescence rate correlated with that of ξ_{ex}. The linear dichroism $\propto (\vec{E} \cdot \hat{\epsilon}_{ex} \wedge \hat{k})(\hat{\epsilon}_{ex} \cdot \vec{B})$ characteristic of a Stark-M_1 interference in the transition rate of a similar highly forbidden Yb transition has also been detected at Berkeley [36] via a change of the fluorescence rate correlated with the direction of the linear polarization of the excitation beam with respect to the fields. The situation is different in pump-probe experiments, *i.e.* our recent APV experiment and those suggested here. The excited state presents some kind of angular anisotropy (alignment [16,22] or orientation, see sect. II and IV) and *the magnetoelectric effect is revealed under the form of a linear or circular dichroism on the forward scattered probe beam.* Probe-beam monitoring is well known in the context of optical pumping [37], but here in the context of highly forbidden transitions it is new to detect the rotational invariants which characterize the Stark interference terms appearing in the forbidden transition probabilities under the form of magnetoelectric optical effects on the probe beam. The advantage is the amplification of these effects occuring while the probe beam propagates through the excited medium with special enhancement when collective effects take place.

VI. CONCLUSION

We have described a new strategy for performing APV measurements in a pump-probe experiment, using detection by stimulated emission following excitation *in transverse electric and magnetic fields.* This method takes advantage of experience gained from our present experiment using a longitudinal E-field, also based on stimulated-emission detection. We have shown that one can circumvent the apparent breaking of rotational symmetry about the propagation axis by rotating the direction of the applied E field.

By using a transverse E field, one could increase both interaction length and field strength without the risk of discharge in a Cs vapour. In this way, optical densities larger than those accessible in the longitudinal field geometry, can provide stronger benefit from the mechanism of asymmetry amplification during propagation of the probe beam in the excited medium. In the limit of quantum noise, one can expect to gain in sensitivity by a factor of 10. Even more favorable conditions can be achieved: by choosing the pump-probe delay to trigger superradiance of the anisotropic excited medium, the left-right asymmetry can be greatly amplified. With these intriguing possiblities, one could look forward to APV measurements at the 0.1% level.

REFERENCES AND NOTES

* e-mail: Marie-Anne.Bouchiat@lkb.ens.fr

[a]Laboratoire Kastler Brossel is a Unité de Recherche de l'Ecole Normale Supérieure et de l'Université Pierre et Marie Curie, associée au CNRS (UMR 8552).

[b]Fédération de Recherche du Département de Physique de l'Ecole Normale Supérieure associée au CNRS (FR684)

[1] M. A. Bouchiat and C. Bouchiat, J. Phys. France, **35**, 899 (1974) and Rep. Prog. Phys. **60**, 1351 (1997), for a complete list of references.

[2] Particle Data Book 2002 (URL: http://pdg.lbl.gov/) 10. Electroweak Model and Constraints on New Physics

[3] V. A. Dzuba, V. V. Flambaum and J. S. M. Ginges **66**, 076013 (2002).

[4] V. A. Dzuba, V. V. Flambaum and O. P. Sushkov, Phys. Lett. A **141**, 147 (1989); S. A. Blundell, J. Sapirstein and W. R. Johnson, Phys. Rev. D **45**, 1602 (1992).

[5] A. Derevianko, Phys. Rev. Lett. **85**, 1618 (2000).

[6] A.I. Milstein and O.P. Sushkov, e-print hep-ph/0109257.

[7] C. S. Wood *et al.*, Science, **275**, 1759 (1997).

[8] S. C. Bennett and C. E. Wieman, Phys. Rev. Lett. **82**, 2484 (1999).

[9] M. A. Bouchiat and J. Guéna, J. Phys. France **49**, 2037 (1988); C. Bouchiat and C. A. Piketty, *J. Phys. France* **49**, 1851 (1988).

[10] W. R. Johnson, M. S. Safronova and U. I. Safronova, Phys. Rev. A **67**, 062106 (2003);

[11] C. Bouchiat and C.A. Piketty, Z. Phys. C **49**, 91 (1991).

[12] M. A. Bouchiat, J. Guéna, L. Hunter and L. Pottier, Phys. Lett. B **117**, 358 (1982); Phys. Lett. B **134**, 463 (1984); J. Phys. (France) **47**, 1709 (1986).

[13] R. Conti, P. Bucksbaum, S. Chu, E.D. Commins and L.R. Hunter, Phys. Rev. Lett. **42**, 343 (1979).

[14] M. A. Bouchiat, Ph. Jacquier, M. Lintz, L. Pottier, Opt. Commun. **56**, 100 (1985).

[15] J. Guéna *et al.*, Phys. Rev. Lett. **90**, 143001 (2003).

[16] M. A. Bouchiat and C. Bouchiat, Z. Phys. D **36**, 105 (1996).

[17] By triggering *several times* the probe beam after each excitation pulse, the photon shot noise on the *reference* measurements can be made negligible and will be ignored.

[18] D. Chauvat *et al.*, Eur. Phys. J. D **1**, 169 (1998).

[19] This, of course, does not hold any longer when the excited medium approaches the conditions of spontaneous superradiance, a situation where spontaneous emission causes additional noise, as discussed in sect. III C.

[20] J. Guéna *et al.*, Quantum Semiclass. Opt. **10**, 733 (1998).

[21] J. Guéna *et al.*, J. Opt. Soc. Am. B **14**, 271 (1997) and Opt. Commmun. **119**, 403 (1995).

[22] M. A. Bouchiat, J. Guéna and M. Lintz, Eur. Phys. J. D, **28**, 331 (2004); e-print arXiv:physics/0311101

[23] For matching the two beam intensities, a simple procedure might rely on a highly parallel glass plate usable as a temperature-tunable Fabry-Perot [24], close to normal incidence on the path of a single beam. The range over which the transmission variation can be adjusted is wide (0 to 15%) and with temperature stabilization stable operating conditions can be achieved.

[24] E. Jahier *et al.*, Appl. Phys. B **71** , 561 (2000).

[25] E. Jahier *et al.*, J. Phys. IV France **12** (2002) Pr5-159; E. Jahier, Thèse de l'Université Paris VI, 2001, (http://theses-en-ligne.in2p3.fr/view-thes-phys-atom_fr.html)

[26] M. A. Bouchiat, J. Guéna and L. Pottier, J. Phys. (France) **46**, 1897 (1985) and **47**, 1175 (1986).

[27] D. G. Sarkisyan, A. V. Melkonyan, Instr. and Exp. Techn. **32**, 485 (1989).

[28] E. Jahier *al.*, Eur. Phys. J. D, **13**, 221 (2001).

[29] For the misalignment of $\vec{E}$ and $\vec{B}$ the measurement principle is based on the detection of the orientation induced by interference between the M_1 and the scalar Stark amplitudes with a single excitation beam and a linear excitation polarization $\propto \mathrm{Re}\{(\hat{E}\cdot\hat{\epsilon}_{ex})(\hat{\epsilon}^*_{ex}\wedge\hat{k})\}$ oriented at 45° of $\vec{B}$. After precession in the $\vec{B}$ field, it gives rise to a longitudinal orientation, that, choosing coordinate axes x and z along $\vec{B}$ and $\hat{k}$, we can write as $\mathrm{Re}\{\epsilon_x\epsilon^*_y\}\delta E_y B_x\hat{k}$. It is odd under the insertion of a $\lambda/2$ plate which reverses the sign of $\mathrm{Re}\{\epsilon_x\epsilon^*_y\}$. Thus, it can easily be compared with the component $|\epsilon_{ex}|^2 E_x B_x\hat{k}$ which is even under this reversal. The ratio between both signals yields directly $<\delta E_y>/E_x$, *i.e.* the misalignment defect.

[30] The transverse and longitudinal field experiments that we consider here differ not only by the field direction, but also by the polarization of the excitation beam, circular versus linear and the hyperfine transitions involved, $6S_{F=4}\rightarrow 7S_{F=4}\rightarrow 6P_{3/2,F=5}$ versus $6S_{F=3}\rightarrow 7S_{F=4}\rightarrow 6P_{3/2,F=4}$. But it turns out that the overall change in the k coefficient is small and can be neglected.

[31] R. H. Dicke, Phys. Rev. **43**, 99 (1954).

[32] L. Mandel and E. Wolf in *Optical Coherence and Quantum Optics*, (Cambridge Univ. Press, 1995) ch.16.

[33] M. Gross and S. Haroche, Phys. Report **93**, 302 (1982).

[34] M. A. Bouchiat, J. Guéna, Ph. Jacquier, M. Lintz and L. Pottier, J. Phys. II France, **2**, 727 (1992); Ph. Jacquier, Thèse d'État, Université de Paris VI (1991).

[35] Hyperfine mixing of the wave functions also contributes to this effect but to a smaller extent, leading to a distortion of the line near the centre (circular dichroism) or in the wings (optical rotation).

[36] J.E. Stalnaker, *et al.*, Phys. Rev. A, **66**, 031403(R) 52002); D. Budker and J. E. Stalnaker, Phys. Rev. Lett.**91**, 263901 (2003).

[37] D. Budker, W. Gawlik, D.F. Kimball, S.M. Rochester, V.V. Yashchuk, A. Weis, Rev. Mod. Phys. **74**, 1153 (2002).